MOLECULAR AND CELLULAR BIOLOGY, Sept. 2005, p. 7734–7742 Vol. 25, No. 17
0270-7306/05/$08.00+0 doi:10.1128/MCB.25.17.7734–7742.2005

Epidermal Growth Factor Receptor Dimerization and Activation Require Ligand-Induced Conformational Changes in the Dimer Interface

Jessica P. Dawson,[1]† Mitchell B. Berger,[1]† Chun-Chi Lin,[2] Joseph Schlessinger,[3] Mark A. Lemmon,[1]* and Kathryn M. Ferguson[2]

Department of Biochemistry and Biophysics[1] and Department of Physiology,[2] University of Pennsylvania School of Medicine, Philadelphia, Pennsylvania, and Department of Pharmacology, Yale University School of Medicine, New Haven, Connecticut[3]

Received 24 January 2005/Returned for modification 17 March 2005/Accepted 13 June 2005

Structural studies have shown that ligand-induced epidermal growth factor receptor (EGFR) dimerization involves major domain rearrangements that expose a critical dimerization arm. However, simply exposing this arm is not sufficient for receptor dimerization, suggesting that additional ligand-induced dimer contacts are required. To map these contributions to the dimer interface, we individually mutated each contact suggested by crystallographic studies and analyzed the effects on receptor dimerization, activation, and ligand binding. We find that domain II contributes >90% of the driving energy for dimerization of the extracellular region, with domain IV adding little. Within domain II, the dimerization arm forms much of the dimer interface, as expected. However, a loop from the sixth disulfide-bonded module (immediately C-terminal to the dimerization arm) also makes a critical contribution. Specific ligand-induced conformational changes in domain II are required for this loop to contribute to receptor dimerization, and we identify a set of ligand-induced intramolecular interactions that appear to be important in driving these changes, effectively "buttressing" the dimer interface. Our data also suggest that similar conformational changes may determine the specificity of ErbB receptor homo- versus heterodimerization.

The epidermal growth factor (EGF) receptor (also designated ErbB) family of receptor tyrosine kinases contains four members: EGFR, ErbB2/HER2, ErbB3/HER3, and ErbB4/HER4 (32). Each mature ErbB receptor contains an extracellular ligand-binding region, a single transmembrane (TM) domain and an intracellular tyrosine kinase domain that is flanked by regulatory regions (30). ErbB receptors are controlled by at least 12 different growth factors including EGF, transforming growth factor α (TGF-α), and the neuregulins. Growth factor binding induces homo- and/or heterodimerization of the receptor, leading to *trans*-autophosphorylation and subsequent activation of SH2 domain-dependent downstream signaling pathways (27).

ErbB receptor signaling is normally very tightly controlled, and its deregulation is linked to several epithelial cancers. Gene amplification, overexpression, and activating mutations of EGFR are seen in glioblastoma, prostate, breast, colorectal, and squamous carcinomas (18, 20, 21, 26). Overexpression of ErbB2 (29) and other ErbB receptors occurs in mammary carcinomas and other human cancers (5). Several anticancer therapies that target ErbB receptors are now being used or tested in the clinic (1), including tyrosine kinase inhibitors (10, 15) and antibodies against ErbB receptor extracellular regions (25).

* Corresponding author. Mailing address: Department of Biochemistry and Biophysics, University of Pennsylvania School of Medicine, 809C Stellar-Chance Laboratories, 422 Curie Boulevard, Philadelphia, PA 19104-6059. Phone: (215) 898-3072. Fax: (215) 573-4764. E-mail: mlemmon@mail.med.upenn.edu.

† J.P.D. and M.B.B. contributed equally to this study.

X-ray crystal structures of ErbB extracellular regions in different activation states have led to a significant advance in our understanding of how receptor dimerization and activation is promoted by growth factor binding (6). Dimerization is driven entirely by receptor-receptor interactions, with a critical "dimerization arm" in the cysteine-rich domain II providing the majority of contacts across the interface (17, 24). Without bound ligand (i.e., in the monomeric receptor) this dimerization arm is buried in an intramolecular "tether" by interacting with domain IV within the same molecule (8, 12), and dimerization of the receptor is thus "autoinhibited" (28). Activating ligands bridge two distinct binding sites on the receptor (in domains I and III) and promote a dramatic domain rearrangement in the extracellular region of the receptor. One key consequence of this rearrangement is disruption of the autoinhibitory intramolecular tether and resulting exposure of the dimerization arm.

Although exposure of the dimerization arm is certainly a critical part of the ErbB receptor activation mechanism, it is not sufficient. Mutations that disrupt the intramolecular domain II or IV tether do not activate EGFR (12, 22, 31). Moreover, deleting domain IV (and thus exposing the dimerization arm) does not cause ligand-independent dimerization of the EGFR extracellular region (11). It is therefore necessary to invoke additional ligand-induced alterations that must promote and stabilize receptor dimerization. Inspection of the EGFR dimer interface (Fig. 1A and B) shows that, although the dimerization arm provides the majority of interactions, several "secondary" receptor/receptor contacts are also made by other parts of domains II and IV (17, 24). We hypothesize that these multiple sites must cooperate with one another (and

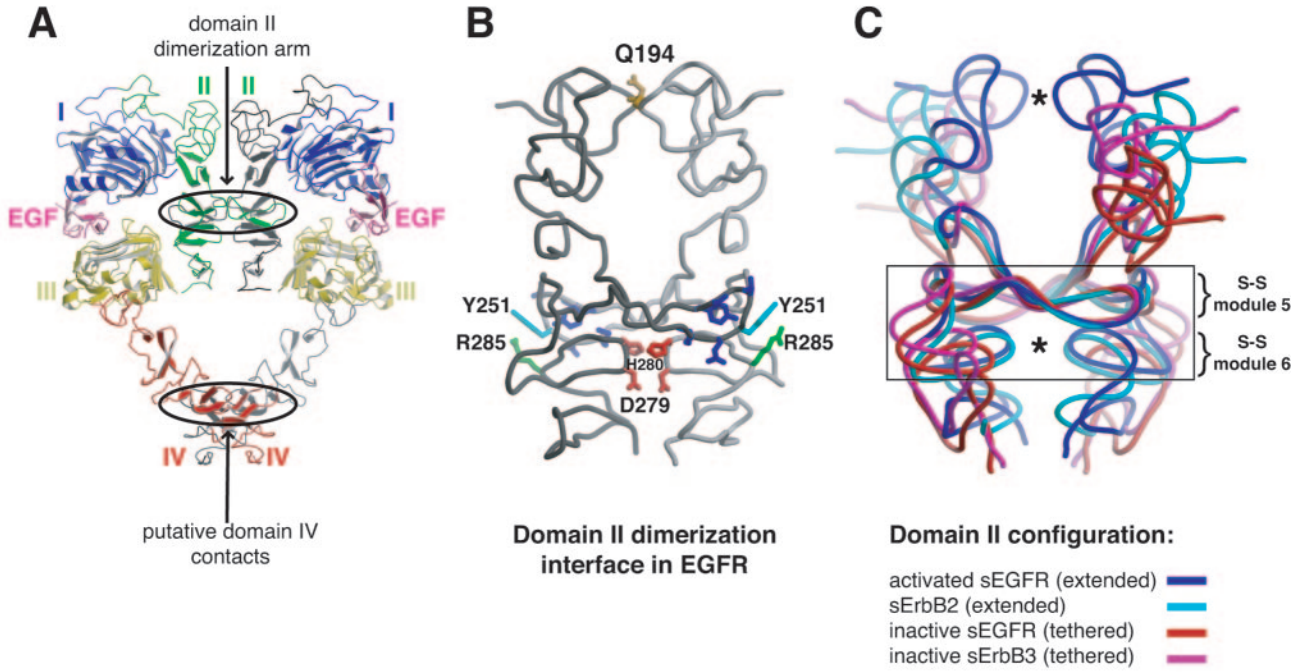

FIG. 1. Contacts across the sEGFR dimer interface. (A) A model for the sEGFR dimer is shown, generated with the coordinates of the EGF/sEGFR complex (24) to which domain IV has been added according to the relationship between domains III and IV in the structure of intact (monomeric) sEGFR (12). This model shows that domain II (green) forms much of the dimer interface and suggests that domain IV (red) may also contribute, as indicated in further crystallographic studies (S. Yokoyama, unpublished data). Domains I, II, III, and IV are labeled, as is bound EGF. (B) A close-up view of domain II from the sEGFR:TGF-α dimer structure (17) as an alpha carbon trace, with domain II of the right-hand protomer shaded light gray and domain II of the left-hand protomer shaded dark gray. The amino acids involved in crystallographically observed dimer contacts are colored. The Q194 side chain (yellow) makes contacts across the interface close to the N terminus of domain II. Residues in the dimerization arm that make intermolecular contacts are dark blue if they were mutated in the 246-253* mutant (Y246, N247, T249, Q252, and M253), green if they were mutated in the Y251A/R285S mutant (R285), and cyan if they were altered in both mutants (Y251). D279 and H280 in disulfide-bonded module 6 are red. (C) Domain II of each protomer from the sEGFR/TGF-α dimer is represented as a dark blue stylized backbone worm. Regions of interface contact (shown in panel B) are denoted by asterisks. Using the dimerization arm as a reference point, we superimposed domain II from each of the other published ErbB receptor structures (8, 9, 12) onto each protomer in the sEGFR dimer. Thus, a copy of domain II from the extended sErbB2 monomer (9) has been superimposed (in cyan) onto each dark blue sEGFR domain II. Similarly, we have superimposed a separate copy of domain II from the sEGFR monomer (red) and the sErbB3 unliganded monomer (magenta) onto each domain II present in the sEGFR dimer. This provides a view of the interactions that each alternate domain II configuration can form across the dimer interface. The region shown in our mutational analysis to contribute >75% of the dimerization energy (disulfide-bonded modules 5 and 6) is boxed. It is apparent that the module 6 contact point (including D279 and H280 in sEGFR) is "withdrawn" from the dimer interface in the red and magenta (monomeric) domain II configurations compared to the position seen in the active configurations (blue and cyan).

with the dimerization arm) to drive efficient receptor dimerization and that ligand binding optimizes this cooperation by altering the relative spatial positions of the sites. Indeed, domain II of dimeric EGFR (blue in Fig. 1C) has a distinct curvature or spine-like bend that allows several contacts across the dimer interface (at the points marked by asterisks) in addition to those involving the dimerization arm. In contrast, the different domain II curvature in monomeric EGFR (red) or ErbB3 (magenta) does not allow these secondary dimerization contacts to be made.

To test our hypothesis and to map the strength of individual contributions to the EGFR dimerization interface, we mutated each crystallographically observed (or implied) dimer contact point and measured the effects on ligand binding and dimerization. Our findings focus attention on the contact point to the immediate C terminus of the dimerization arm (lower asterisk in Fig. 1C) and argue that ligand binding induces a local conformational change in this region that is essential for the generation of a self-complementary dimer interface. These results explain why simple exposure of the dimerization arm is insufficient for receptor activation and have interesting implications for understanding the specificity of ErbB receptor heterodimerization.

MATERIALS AND METHODS

Mutagenesis and protein purification. All mutations were introduced by using the Stratagene QuikChange system according to the manufacturer's recommendations, and sequences were confirmed by standard procedures. Wild-type and mutated forms of soluble EGFR extracellular region (sEGFR) were produced from Sf9 cells infected with the relevant recombinant baculoviruses and were purified exactly as described previously (13). Recombinant EGF and TGF-α were purchased from Chemicon International (formerly Intergen, Inc.) and were used without further purification.

SPR. EGF and TGF-α binding by sEGFR variants was analyzed by surface plasmon resonance (SPR), using a Biacore 3000 instrument as described previously (12). All experiments were performed in degassed 25 mM HEPES buffer (pH 8.0) containing 150 mM NaCl, 3 mM EDTA, and 0.005% Surfactant P-20 at 25°C. EGF and TGF-α were immobilized on a Biacore CM5 biosensor chip by amine coupling as follows: the CM-dextran matrix was activated with 1-ethyl-3(3-diethylaminopropyl)-carbodiimide hydrochloride (EDC) and *N*-hydroxysuc-

TABLE 1. Ligand binding affinities for sEGFR mutants measured using SPR (Biacore)

sEGFR mutant	K_D (nM)		Region mutated[a]
	EGF	TGF-α	
sEGFR wt	175 ± 5.8	353 ± 16	
Q194A	162 ± 4.0	306 ± 16	Domain II interface
Y251A/R285S	832 ± 50	1,125 ± 70	Domain II interface
D279A/H280A	877 ± 156	1,677 ± 166	Domain II interface
246-253*	260 ± 12	357 ± 43	Domain II interface + tether
563/566/585*	50 ± 5	83 ± 8	Domain IV interface + tether
Δ575-584	32 ± 2	51 ± 5	Domain IV interface + tether
sEGFR501	7.8 ± 3.1	13.6 ± 5.2	Domain IV interface + tether

[a] The domain IV interface was inferred from models.

TABLE 2. Estimated K_D values for dimerization of each sEGFR mutant in a 1:1 sEGFR/TGF-α complex

sEGFR mutant	Dimerization K_D (μM)	Region mutated[a]
sEGFR wt	1.2 ± 2.6	
Q194A	7.4 ± 5.8	Domain II interface
Y251A/R285S	–[b]	Domain II interface
D279A/H280A	147 ± 101	Domain II interface
246-253*	–	Domain II interface + tether
563/566/585*	3.8 ± 4.3	Domain IV interface + tether
Δ575-584	4.3 ± 2.1	Domain IV interface + tether
sEGFR501	3.6 ± 2.1	Domain IV interface + tether

[a] The domain IV interface was inferred from models.
[b] –, no dimerization.

cinimide. Growth factor (at 200 μg/ml in 10 mM sodium acetate [pH 4.0]) was then flowed over the activated surface at 5 μl/min for 10 min. Non-cross-linked ligands were removed, and the remaining reactive sites were blocked with 1 M ethanolamine-HCl. Immobilized EGF contributed a signal of 212 response units (RU) and TGF-α contributed 171 RU.

Purified sEGFR proteins at a series of concentrations were flowed over the EGF and TGF-α surfaces (as well as a control surface with no immobilized ligand) at 10 μl/min for 10 min (which was sufficient time for binding to reach a plateau), and the surfaces were then washed with buffer between injections to bring RU values to baseline. The only exceptions were the sEGFR501, Δ575-584, and 563/566/585* mutants (which have disrupted tethers and so dissociate more slowly), which were flowed over the surface for 20 min and subjected to a regeneration-wash injection (10 mM sodium acetate, 1 M NaCl [pH 5.2]) between samples to return the RU to baseline. The RU signal corresponding to the height of the plateau was background corrected by subtracting the signal obtained with the control surface from that measured with EGF or TGF-α. Steady-state/plateau RU values then were plotted against sEGFR concentrations in GraphPad Prism 4 (GraphPad Software, Inc., San Diego, CA) and fit to a simple single-site saturation binding model as previously described (13), in order to estimate the apparent dissociation constants (K_D) listed in Table 1. Each experiment was performed at least in triplicate, and the standard deviation of the mean K_D value is quoted.

Analytical ultracentrifugation studies. Ligand-induced dimerization of the sEGFR variants was analyzed by sedimentation equilibrium experiments using an XL-A analytical ultracentrifuge (Beckman, Fullerton, CA). Samples (10, 5, and 2 μM) of wild-type or mutated sEGFR protein were analyzed both in the presence and in the absence of a 1.2-fold molar excess of TGF-α. Since the only 280-nm-absorbing group in TGF-α is a single tyrosine [ε_{280}(TGF-α) ≈ 1,490/M/cm, while ε_{280}(sEGFR) = 57,620/M/cm], TGF-α contributes insignificantly (~3%) to the 280-nm absorbance of our centrifugation samples.

All experiments were performed in 25 mM HEPES–150 mM NaCl (pH 8.0), which was also used as a buffer blank. Samples were loaded in six-channel charcoal-Epon cells with quartz windows at both ends. Radial scans were performed at 20°C at 6,000, 9,000, and 12,000 rpm in an An Ti 60 rotor, with detection over a wavelength range of 236 to 285 nm. The partial specific volume of sEGFR proteins was estimated as 0.71 ml/g as before (13), and solvent density was taken as 1.003 g/ml. Monomeric molecular masses were determined by fitting multiple data sets (obtained at 10 μM for three different speeds) for ligand-free sEGFR to a simple model for a single, nonideal, species in Origin (OriginLab Corp., Northampton, MA).

To estimate K_D values for sEGFR dimerization, we assumed that all sEGFR in the sample was occupied with TGF-α in a 1:1 complex, so that neither free TGF-α nor free sEGFR contribute significantly to the 280-nm absorbance of the sample. Using this assumption, we fit multiple datasets (three concentrations at three speeds) to a model describing simple dimerization of a 1:1 sEGFR/TGF-α complex, in order to obtain a first approximation of the dimerization strength: $A_r = A_0\exp[H \cdot M(r^2 - r_0^2)] + A_0^2 \cdot K_a\exp[H \cdot 2M(r^2 - r_0^2)]$, where A_r is the absorbance at radius r, A_0 is the absorbance at the reference radius r_0, M is the molecular weight of the 1:1 sEGFR/TGF-α complex (the sum of the measured monomeric sEGFR and TGF-α molecular weights), H is the constant $[(1 - \nabla\rho)\omega^2]/2RT$, ∇ is the partial specific volume (estimated at 0.71 ml/g), ρ is the solvent density (1.003 g/ml), ω is the angular velocity of the rotor (radians/sec), R is the gas constant, T is the absolute temperature, and K_a is the fitted parameter corresponding to the equilibrium concentration for dimerization of the 1:1 sEGFR/TGF-α complex.

The fitted K_a value is converted to the dissociation constant K_D ($K_D = 1/K_a$) reported in Table 2 by using the extinction coefficient for the 1:1 sEGFR/TGF-α complex determined from values listed above. At least three independent groups of experiments were performed and fit for each mutated protein, and estimated K_D values are quoted as the mean ± the standard deviation of the estimates from individual experiments.

Receptor activation at the cell surface. Each mutation of interest was also introduced into full-length EGFR subcloned into the vector pAc5.1/V5-HisA (Invitrogen Corp., Carlsbad, CA) for expression in *Drosophila melanogaster* Schneider-2 (S2) cells as previously described (4). S2 cells were transfected with the relevant vector (plus pCoHygro selection vector) and selected exactly as described previously (4). Stable pools of EGFR-expressing cells were maintained in complete Schneider's medium supplemented with 10% fetal bovine serum (FBS) and 300 μg of hygromycin B/ml.

For fluorescence-activated cell sorting (FACS) analysis, cells were harvested and blocked in ice-cold phosphate buffered saline (PBS) containing 2% FBS (vol/vol) and 100 mM EDTA (pH 8.0; FACS buffer) for 15 min on ice. A total of 10^6 cells were then resuspended in 100 μl of ice-cold FACS buffer and incubated for 30 min on ice with 40 μl of R-phycoerythrin-conjugated anti-EGFR antibody (Pharmingen, San Diego, CA). Solutions were finally diluted to ca. 500 μl in FACS buffer. Flow cytometry was performed by using a FACScan flow cytometer (BD Biosciences).

To analyze ligand-induced EGFR phosphorylation, ca. 10^7 S2 cells expressing each EGFR variant were harvested, washed in PBS, and incubated in serum starvation media (containing just 0.5% FBS) overnight. Cells were then stimulated on ice for 10 min, by adding 100 ng of EGF or TGF-α/ml (unstimulated cells were incubated on ice for 10 min with no added growth factor). Cells were then pelleted, washed in ice-cold PBS, and lysed with ice-cold radioimmunoprecipitation assay buffer (25 mM Tris-HCl [pH 7.5], containing 150 mM NaCl, 1% Triton X-100, 1% sodium deoxycholate, 0.1% sodium dodecyl sulfate, 1 mM phenylmethylsulfonyl fluoride, 1 μg of leupeptin/ml, 1 μg of aprotinin/ml, 25 mM NaF, 5 mM Na_2MoO_4, and 0.2 mM Na_3VO_4). Lysates were clarified by centrifugation at 14,000 rpm for 10 min at 4°C, and protein concentrations in the supernatants were determined by using the Bio-Rad protein assay (Bio-Rad, Hercules, CA) to allow normalization of protein levels.

Samples of equal protein levels were boiled, separated by sodium dodecyl sulfate-polyacrylamide gel electrophoresis (SDS-PAGE), and transferred to nitrocellulose membranes. Immunoblotting was performed with anti-EGFR antibody Ab-15 (NeoMarkers, Freemont, CA) and antiphosphotyrosine antibody PY20 (Zymed Laboratories, South San Francisco, CA), plus horseradish peroxidase-conjugated secondary antibodies for detection. Western blots were developed by using SuperSignal West Pico Chemiluminescent Substrate (Pierce Biotechnology, Rockford, IL) and an Image Station 440CF (Eastman Kodak Company, New Haven, CT).

RESULTS AND DISCUSSION

Our primary goal was to "map" the relative contribution to receptor dimerization of each intermolecular contact point

observed in (or implied from) X-ray crystal structures of the dimeric EGFR extracellular region (17, 24). Using site-directed mutagenesis, we individually disrupted each dimer contact point contributed by domain II (Fig. 1B) and all potential domain IV contacts (Fig. 1A).

Domain II mutations. The sites of domain II contact across the dimer interface are detailed in Fig. 1B. At the top of this representation, the Q194 side chain (yellow) makes a hydrogen bond across the interface and buries 225 Å^2 of surface area (17). To disrupt this contact, we mutated Q194 to alanine. Moving down domain II, the next contact point is the most extensive part of the dimer interface (burying $>$ 800 Å^2), centered on the dimerization arm. We disrupted this interaction in two ways. In one mutated form of the receptor (similar to that made by Garrett et al. [17]) we made six substitutions in the dimerization arm (Y246E, N247A, T249D, Y251E, Q252A, and M253D; blue or cyan in Fig. 1B), to give the 246-253* mutant. In a second mutated form, Y251 and R285 (cyan and green in Fig. 1B) were replaced with alanine and serine, respectively (Y251A/R285S), to disrupt an interreceptor hydrogen bond pointed out by Ogiso et al. (24). The remaining intermolecular contact made by domain II (17) involves D279 and H280 (colored red in Fig. 1B), which are at the tip of a loop that emanates from the sixth disulfide-bonded module of domain II. This contact point, immediately C terminal to the dimerization arm, was disrupted in a D279A/H280A double mutant.

Domain IV mutations. Domain IV has also been suggested to contribute significantly to EGFR dimerization, as illustrated in the dimer model shown in Fig. 1A (12). Domain IV contacts across the sEGFR dimer interface have been observed crystallographically (6; S. Yokoyama, unpublished data), and peptide mimetics corresponding to the C terminus of domain IV reportedly interfere with ErbB receptor homo- and heterodimerization (3). To disrupt these proposed interactions, we deleted most (~85%) of domain IV (residues 502 to 618) to generate a truncated form of the EGFR extracellular region (sEGFR501) that has previously been well studied (11, 17). We also made an sEGFR variant in which a prominent loop was deleted from the fifth disulfide-bonded module of domain IV (to give Δ575-584). This loop, which extends from V575 to W584, interacts with the dimerization arm in the tethered sEGFR structure (12) and was proposed as a second putative dimerization arm in domain IV (Fig. 1A) (3, 12). Finally, we included in this analysis an sEGFR variant that we described previously (12) in which residues 563, 566, and 585 in domain IV were mutated to alanine (563/566/585*), thus disrupting the intramolecular domain II/IV tether in the EGFR monomer. Except for sEGFR501 (which was only analyzed in vitro), each set of mutations was made both in the context of the isolated EGFR extracellular region (for in vitro biophysical studies of sEGFR) and in the intact receptor (for analysis of receptor activation at the cell surface).

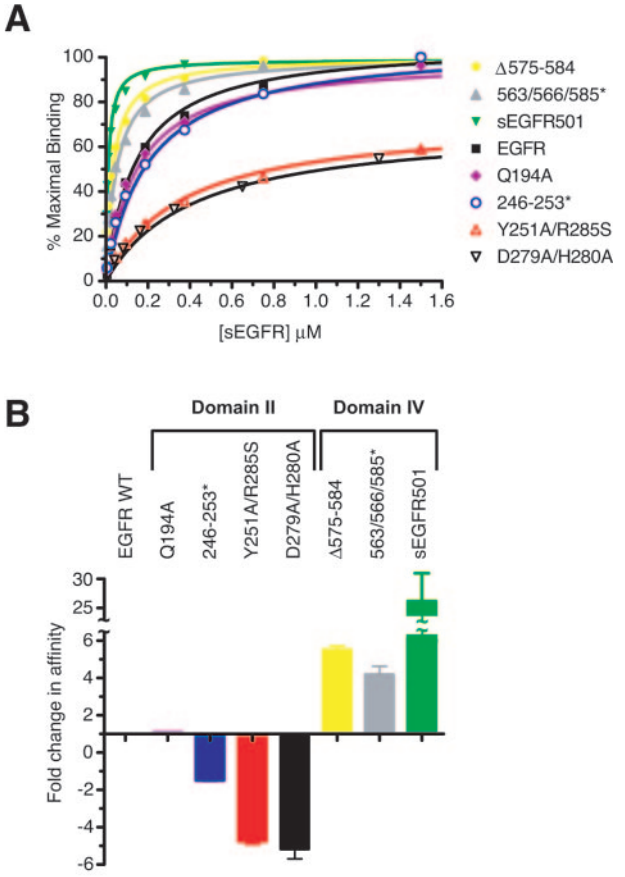

FIG. 2. Effects of mutations and deletions on ligand binding by sEGFR, assessed by using SPR. (A) Mean best-fit binding curves for binding of each sEGFR mutant to immobilized EGF are plotted, together with data points for a representative experiment (at least three independent experiments were performed for each analysis). Mutants that bind EGF with an affinity that is equal to (or greater than) that of the wild-type sEGFR are represented by solid data points, while those that bind more weakly than wild-type are represented with open data points, according to the key provided in the figure. The Y251A/R285S and D279A/H280A mutants, which are the weakest binders, at sEGFR concentrations of ~10 μM, do reach saturation giving binding signals that are 94% (2,130 RU) and 98% (2,230 RU) of maximal wild-type binding for the Y251A/R285S and D279A/H280A mutants, respectively. (B) A bar graph summarizes the relative affinities of each sEGFR mutant for immobilized EGF. The wild-type sEGFR is set at a value of 1. Values for mutated forms of sEGFR are reported as a fold increase (positive values) or decrease (negative values) in affinity. For example, with a K_D(EGF) of 877 nM, the D279A/H280A mutant binds EGF fivefold more weakly than does the wild type (K_D = 175 nM), giving a fold change in affinity of −5. In contrast, with a K_D(EGF) of 7.8 nM, sEGFR501 binds EGF 22-fold more strongly than does the wild type, giving a fold change in affinity of +22. Error bars represent the standard deviation for at least three separate measurements, as reported in Table 1.

Effects of mutations on ligand binding. We first assessed the effect of each set of mutations on ligand binding to the purified EGFR extracellular region (sEGFR). We used SPR to analyze binding to EGF and TGF-α that had been immobilized on CM5 Biacore biosensor chips (see Materials and Methods). The results are summarized in Fig. 2 and Table 1. None of the variants showed dramatically reduced ligand-binding affinity (or altered production and purification properties), arguing that none of the mutations simply compromise protein folding. Three of four domain II dimerization-site mutants showed slightly reduced ligand-binding affinity, by between 1.5 and 5-fold (with D279A/H280A having the lowest affinity), suggesting that impaired dimerization may lead to compromised ligand binding, as expected since ligand binding and dimeriza-

tion are thermodynamically coupled. Mutation of Q194 to alanine had no detectable effect on ligand binding, suggesting that this dimer contact may not be important. Further consideration of the effects of these domain II mutations on ligand binding requires knowledge of their effects on dimerization, which is described in the next section.

In contrast to the domain II substitutions, all of our domain IV mutations increased ligand-binding affinity, which we interpret to be a consequence of reducing the intramolecular domain II/IV tether strength. The 563/566/585* triple mutation (which breaks three hydrogen bonds in the tether) increased affinity for EGF and TGF-α by ~4-fold compared to wild type (Table 1). We previously ascribed this effect to an ~0.8 kcal/mol weakening of the domain II/IV tether in sEGFR (12) that resists bringing domains I and III sufficiently close for them both to bind the same ligand molecule. The domain IV loop comprising residues 575 to 584 also contributes to the domain II/IV tether in monomeric sEGFR, through van der Waals interactions plus at least one backbone hydrogen bond (12). As expected, the Δ575-584 mutation also enhances ligand binding affinity, by ~6-fold, suggesting a contribution to the intramolecular tether from these residues of ~1.1 kcal/mol. Consistent with these values, deletion of residues 502 to 618 (most of domain IV) in sEGFR501 increases ligand binding affinity by ~24-fold (Table 1), suggesting that the total energy of the domain II/IV tether is ~1.9 kcal/mol. These findings suggest that residues 563/566/585 (which contribute 0.8 kcal/mol) and 575 to 584 (which contribute 1.1 kcal/mol) together make up the complete set of tether interactions in sEGFR.

It should be noted that the 246-253* mutation in domain II has dual effects. It impairs dimerization (see below), leading to reduced ligand-binding affinity. However, it also disrupts the intramolecular tether (which increases ligand-binding affinity). The net effect of these two opposing influences causes this mutant to bind TGF-α indistinguishably from wild-type sEGFR (although EGF binding affinity is slightly reduced).

Effects of mutations on sEGFR homodimer formation. To determine how efficiently each mutated form of the EGFR extracellular region dimerizes, we used sedimentation equilibrium analytical ultracentrifugation as previously described (13). First, we established that none of the mutations promotes constitutive sEGFR dimerization. In the absence of added ligand, each altered protein sedimented as a single nonideal species with an estimated molecular mass close to the value predicted from its sequence (with assumed glycosylation). Thus, sEGFR501 sedimented as a species of 60.9 ± 0.3 kDa, while all other sEGFR variants behaved as species with masses between 75 and 80 kDa. These results confirm previous reports that disrupting the intramolecular domain II/IV tether (and thus exposing the dimerization arm) is not sufficient to promote ligand-independent EGFR dimerization (11, 12, 17, 22, 31).

The ability of each mutated form of sEGFR to dimerize upon ligand binding is summarized in Fig. 3. Each graph shows a plot of the natural logarithm of the absorbance at 280 nm (proportional to protein concentration) against a function of the square of the radial position in the sample (with or without added TGF-α). Analytical ultracentrifugation data for any single species gives a straight line in this representation, with slope proportional to the molecular mass of the species (7).

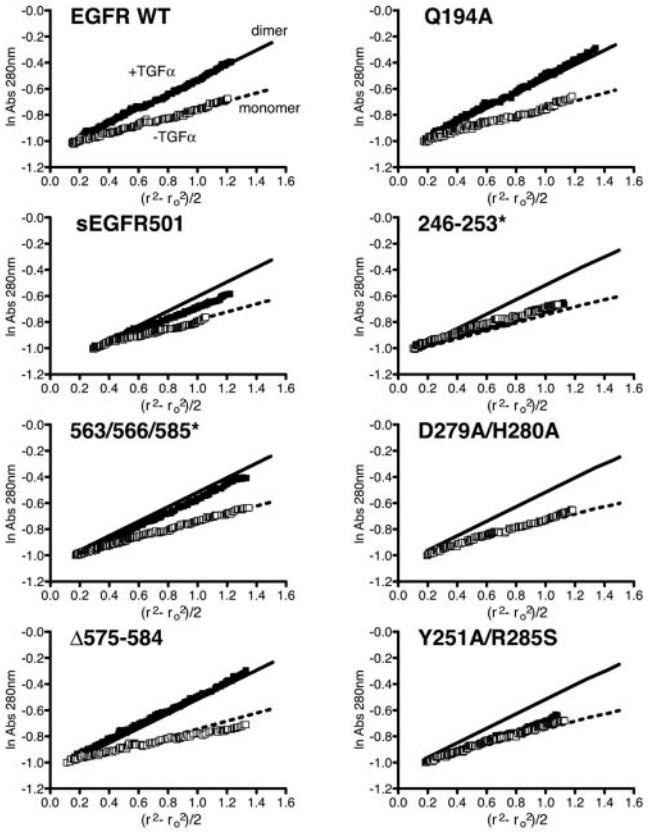

FIG. 3. Analysis of TGF-α-induced dimerization of sEGFR mutants using sedimentation equilibrium analytical ultracentrifugation. Raw analytical ultracentrifugation data are plotted as the natural logarithm (ln) of absorbance at 280 nm against a function of the radius squared $(r^2 - r_o^2)/2$, where r is the radial position in the sample and r_o is the radial position of the meniscus. For a single species, this representation gives a straight line with slope proportional to its molecular mass. The data are shown for experiments run with an sEGFR concentration of 10 μM, with or without the addition of 12 μM TGF-α, and at a rotor speed of 6,000 rpm. For each protein, data obtained with added ligand are represented by filled squares, and data obtained without added ligand are represented by open squares. For wild-type sEGFR, best-fit straight lines for the data are shown with TGF-α (solid black line), corresponding to dimer (as marked) or without TGF-α (broken black line), corresponding to monomer (as marked). These same straight lines are superimposed on all other plots in the figure, as representative results for a dimerizing and nondimerizing sEGFR molecule. Estimates of dimerization K_D values for a 1:1 sEGFR/TGF-α complex, from a more complete analysis of the data (see Materials and Methods), are listed in Table 2.

Addition of TGF-α (at a 1.2-fold molar excess) should not affect the slope of this line unless it promotes sEGFR oligomerization. The added TGF-α (with one tyrosine and no tryptophans) contributes negligibly (<3%) to the absorbance of the sample at 280 nm. Moreover, with a molecular mass of just 5.6 kDa, stoichiometric binding of TGF-α to an sEGFR monomer will only increase the sEGFR molecular mass by ~7%, which would barely be detectable in this representation. The fact that the slopes of the straight lines for wild-type sEGFR and sEGFR501, as well as the 563/566/585*, Δ575-584, and Q194A mutants, all approximately doubled upon addition of TGF-α (compare filled and open symbols in Fig. 3) shows

that each of these proteins dimerizes upon ligand binding. In contrast, this qualitative assessment shows that the dimerization arm mutations (246-253* and Y251A/R285S) and the D279A/H280A mutation impair ligand-induced sEGFR dimerization. This lack of dimerization cannot arise from the relatively minor reduction in ligand binding affinity reported in Table 1 for each mutant. Under the conditions used for the experiment shown in Fig. 3 (with 10 μM sEGFR and 12 μM TGF-α) an increase in the K_D of ligand binding from 0.3 μM to 1.1 or 1.7 μM should not have a significant impact on the extent to which the receptor is occupied with ligand, so this is highly unlikely to explain the dramatic effects of the 246-253*, Y251A/R285S, and D279A/H280A mutations on sEGFR dimerization.

Relative strengths of sEGFR dimerization. For a more quantitative analysis of dimerization, we globally fit datasets obtained at multiple speeds and protein concentrations for each mutated form of sEGFR to a simple dimerization model. We ignored the absorbance of free ligand; this guided our choice of poorly UV-absorbing TGF-α for these experiments. We also assumed that all sEGFR in the sample was occupied with TGF-α, since we used an excess (1.2-fold) of the ligand and, for most samples, used sEGFR and TGF-α concentrations in excess of five times K_D for ligand binding. Although only strictly correct to a first approximation, these assumptions allowed us to fit all of our data straightforwardly to a model that involves simple dimerization of a 1:1 sEGFR/TGF-α complex (see Materials and Methods) and thus to estimate K_D values for each mutant for this dimerization event. Fits to the data using this model consistently gave good residuals, with no systematic deviations.

The approximate K_D values obtained using this approach for dimerization of a 1:1 sEGFR/TGF-α complex are listed in Table 2. For wild-type sEGFR, we estimated a K_D of ~1.2 ± 2.6 μM ($\Delta G = -8.1$ kcal/mol), which is consistent with values (2.4 to 3.3 μM) previously measured using other approaches (19, 23). Mutating Q194 to alanine reduced dimerization affinity by ~6-fold (K_D of ca. 7.4 ± 5.8 μM), arguing that this side chain does not contribute more than approximately 1 kcal/mol to the energy of dimerization (~12% of the total 8.1 kcal/mol).

Neither the 246-253* dimerization arm mutant nor the Y251A/R285S mutant showed any detectable dimerization. As mentioned above, the D279A/H280A mutation significantly disrupted (but did not completely abolish) sEGFR dimerization (Table 2), and the best fits to the data were obtained with a K_D value for dimerization of ca. 150 μM (120 times weaker than wild type). These sites therefore represent key parts of the dimer interface.

Contrary to our expectations, deletion of domain IV (in sEGFR501) had only a very small, insignificant, effect on dimerization strength ($K_D \approx 3.6 \pm 2.1$ μM), arguing that domain IV can contribute no more than 0.7 kcal/mol to the strength of the sEGFR dimer interface (~9%). Similar results were obtained for the 563/566/585* mutant ($K_D \approx 3.8 \pm 4.3$ μM) and the Δ575-584 mutant ($K_D \approx 4.3 \pm 2.1$ μM), which is consistent with the observation that the C terminus of domain IV does make contact across the dimer interface (6), but again indicating that domain IV does not contribute substantially to stabilization of the sEGFR dimer. It should be noted that this result is not consistent with a report by Berezov et al. (3) that cyclic peptides modeled on the C-terminal disulfide-bonded modules of domain IV can bind ErbB receptor extracellular regions and inhibit receptor signaling. A contribution by domain IV of just 1 kcal/mol to sEGFR dimerization is consistent with a K_D of ~180 mM for dimerization of isolated domain IV (or peptides), which would not be measurable. Moreover, our Δ575-584 mutation, which has little effect on sEGFR dimerization (or EGFR activation [see below]), removes several of the residues contained in the EGFR cyclic peptide used by Berezov et al. (3). The origin of the reported effects of these peptides is therefore not clear from our studies.

Our analysis of the sEGFR dimerization interface focuses attention on both the dimerization arm—already known to be critical for EGFR dimerization—and the loop containing D279 and H280 (in disulfide-bonded module 6), which we find also plays an unexpected critical role. Other parts of domain II (or domain IV) do not contribute significantly to the energy of dimerization.

Effects of dimer interface mutations on activation of intact EGFR at the cell surface. To determine whether the mutations studied here have the same effect on EGFR activation at the cell surface as they do on sEGFR dimerization in vitro, we introduced each of them into the intact receptor. The resulting mutated forms of human EGFR were expressed in *Drosophila* Schneider 2 cells as a null background. Cell surface expression of each altered receptor was confirmed by FACS analysis (Fig. 4A), which also showed that our pools of EGFR-expressing cells sample a wide range of receptor expression levels. The ability of EGF and TGF-α to induce tyrosine autophosphorylation of mutated EGFR (Fig. 4B) correlated very well with the effects of the equivalent mutations on sEGFR dimerization in vitro. Thus, autophosphorylation of the Q194A and Δ575-584 mutants (for which sEGFR dimerizes with K_D values of 7.4 and 4.3 μM) was indistinguishable from wild-type EGFR (dimerization K_D of ~1.2 μM). In contrast, autophosphorylation of the D279A/H280A mutant (dimerization K_D in vitro of ~150 μM) was barely detectable, even with saturating ligand concentrations. No activation at all could be seen for the dimerization arm mutants (246-253* or Y251A/R285S), in agreement with previous reports (17, 24). Also in agreement with other studies (12, 22, 31) and our biophysical analysis, mutations that disrupt the intramolecular domain II/IV tether did not cause constitutive activation/dimerization of the receptor. Neither the Δ575-584 mutant nor the 563/566/585* mutant, which both have a compromised intramolecular tether, showed any sign of constitutive activation (Fig. 4B and data not shown) or enhanced EGF sensitivity in ligand dose-response analyses at the cell surface.

The conformation of the dimer interface is stabilized by ligand-induced domain II/III interactions. Our mutational analysis shows that the domain II dimerization arm (in disulfide-bonded module 5 [see Fig. 5A]) and a single adjacent loop containing D279 and H280 (in disulfide-bonded module 6) together contribute more than 75% of the sEGFR dimerization energy. As shown in Fig. 1C, ligand binding is associated with a significant change in the relative positions of these two disulfide-bonded modules. The D279/H280 loop (module 6) appears to be projected toward the center of the dimer interface (at the asterisk) in dimeric sEGFR (blue in Fig. 1C) and

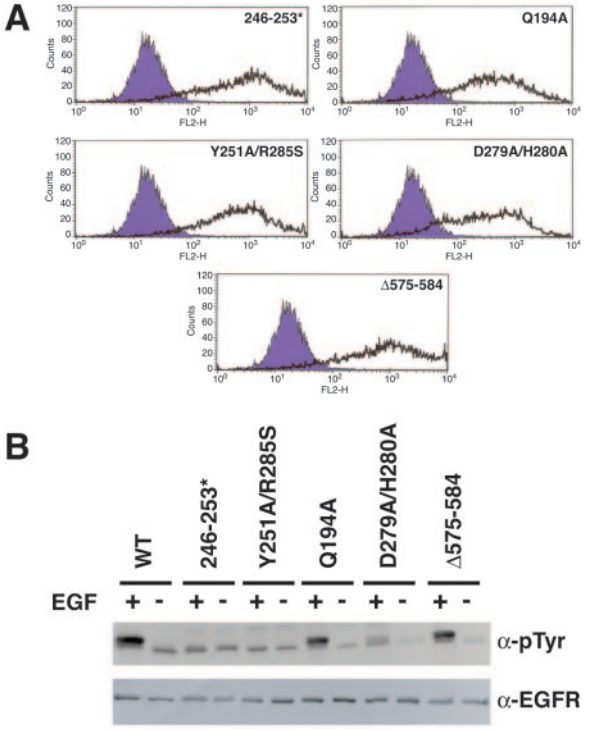

FIG. 4. Analysis of ligand-activation of intact EGFR mutants. (A) Pools of S2 cells expressing full-length EGFR mutants were analyzed by FACS as described in Materials and Methods. The filled traces represent data from control parental S2 cells treated with a phycoerythrin-conjugated antibody against the EGFR extracellular region, while the open traces represent data from the transfected stable cell pools analyzed in the same fashion. The marked right shift in each case demonstrates that each chimera is expressed appropriately at the cell surface and that our pools sample a wide-range of expression levels. A total of 10,000 cells were analyzed for each FACS analysis. (B) S2 cells stably expressing the noted EGFR mutants were serum starved overnight and then chilled and left unstimulated (−) or treated with 100 ng of EGF/ml on ice for 10 min. Receptor autophosphorylation in normalized whole-cell lysates was analyzed by immunoblotting with antiphosphotyrosine (α-pTyr) antibody (upper blot) and an antibody specific for the EGFR intracellular domain (α-EGFR) (lower blot). Similar studies with TGF-α gave identical results. Studies to assess the dependence on EGF concentration of phosphorylation of the Δ575-584 mutant showed no difference from the wild type.

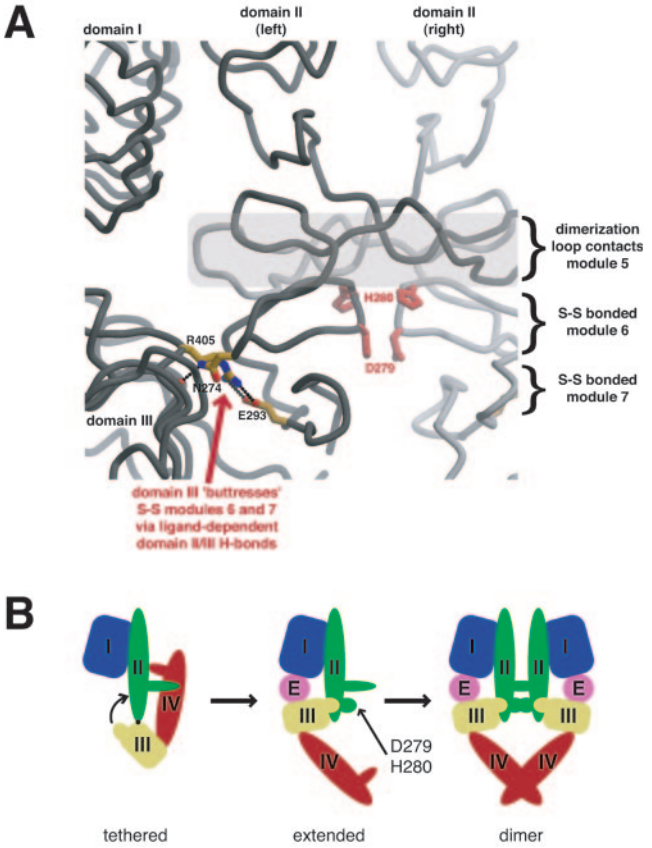

FIG. 5. Domain III "buttresses" the C terminus of domain II for participation in the dimer interface. (A) In the structure of the ligand-bound sEGFR dimer, a "buttressing" interaction of domain III with the "back" of domain II sets up contacts across the dimer interface. A close-up view of domain II in the interface of the sEGFR/TGF-α dimer is shown (17), with the positions of domains I and III marked at the left. The contact region involving D279 and H280 (in disulfide-bonded module 6) is indicated with red side chains, and the dimerization arm region (in disulfide-bonded module 5) is marked with a transparent gray box. In the ligand-activated conformation, domain III lies against the "back" of domain II and interacts with the face of domain II that projects away from the dimer interface. The side chain from R405 of domain III forms a salt bridge with E293 from module 7 of domain II. Simultaneously, the side chain of N274 (from module 6 of domain II) forms a hydrogen bond with the domain III backbone. These hydrogen-bonds and salt bridges are marked and appear to "buttress" modules 6 and 7 of domain II so that the D279/H280 loop of module 6 is projected further into the dimer interface to make contact with the adjacent receptor molecule. (B) Upon ligand binding to the tethered (monomeric) form of sEGFR, domain III is swung from the position shown in the left-hand panel of this diagram (where it is held by the domain II/IV tether) into a position where it lies against the back of domain II, allowing the buttressing interactions shown in detail in panel A. This movement of domain III occurs about an axis represented by the black circle between domains II and III and is depicted with a curved arrow. The position of R405 in domain III is represented by an (exaggerated) protrusion from domain III that is shown projecting into domain II when swung into position and buttressing the critical dimer contacts, including those mediated by D279 and H280. This dimer contact is depicted as an (exaggerated) ligand-induced projection from the C-terminal part of domain II that makes contact across the dimer interface in the right-hand part of the figure.

relatively withdrawn from the interface in monomeric sEGFR (red in Fig. 1C). Ogiso et al. (24) pointed out several hydrogen bonds between domains III and II in the ligand-induced sEGFR dimer that could be responsible for this change and may therefore be critical for receptor dimerization. As shown in Fig. 5A, the N274 side chain from module 6 of domain II hydrogen bonds with the backbone of domain III. There is also a salt bridge between the E293 side chain (from module 7 of domain II) and R405 in domain III. None of these interactions can occur in the tethered sEGFR configuration because the domain II/IV tether effectively "pulls" domain III away from the back of domain II, as depicted schematically in Fig. 5B. However, when EGF or TGF-α binds simultaneously to domains I and III of sEGFR, domain III is moved into a position where it contacts the "back" of domain II, as depicted in moving from the left-hand panel to the center of Fig. 5B.

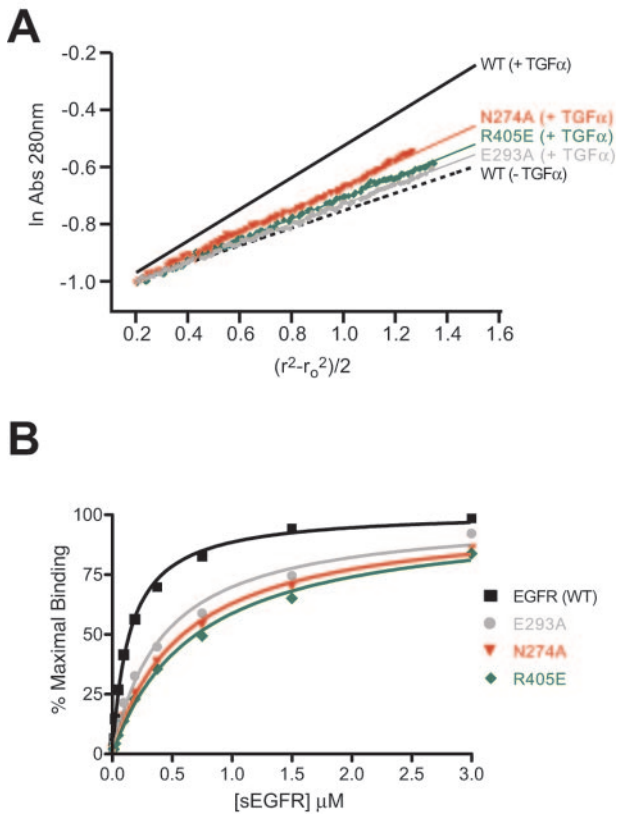

FIG. 6. Effects of buttress mutations on ligand binding and receptor dimerization. (A) Raw analytical ultracentrifugation data are plotted as described for Fig. 3 for TGF-α-bound N274A, R405E, and E293A mutants of sEGFR. For comparison, solid and dashed lines from Fig. 3 for wild-type sEGFR dimer (+TGF-α) and monomer (−TGF-α), respectively, are also plotted. TGF-α-induced dimerization of E293A and R405E sEGFR was essentially undetectable, whereas the N274A mutant gave an approximate K_D of 50 μM. (B) Representative curves from SPR experiments are shown for binding of each sEGFR buttressing mutant to immobilized EGF. All three mutants showed ~4-fold-reduced binding affinity compared to the wild type. For EGF binding, apparent K_D values were 555 ± 43 nM for N274A, 472 ± 31 nM for E293A, and 671 ± 25 nM for R405. For TGF-α binding, the apparent K_D values were 1,420 ± 150 nM for N274A, 1,332 ± 104 nM for E293A, and 1,470 ± 93 nM for R405. Three independent experiments were performed for each analysis.

Through the interactions detailed in Fig. 5A, domain III in this position may "buttress" both module 6 (through the hydrogen bond with N274) and module 7 (through salt bridge formation with E293) and effectively push these two modules (and thus D279 and H280) further into the dimerization interface so that they promote receptor association. In support of this model, Ogiso et al. reported that an R405E mutation in intact EGFR prevents it from being activated by EGF (24).

To further test this hypothesis, we individually mutated each of the putative buttressing residues N274, E293, and R405, and analyzed ligand binding and dimerization for each mutated sEGFR protein. As shown in Fig. 6A, the E293A or R405E sEGFR mutants failed to dimerize significantly upon addition of TGF-α when assessed by analytical ultracentrifugation. The N274A mutant showed some evidence of dimerization, but gave a mean dimerization K_D value of ~50 μM from global fits of multiple experiments (compared to 1.2 μM for wild-type sEGFR). To exclude the trivial possibility that these mutations simply prevent ligand binding, we assessed their binding to EGF and TGF-α by using SPR (Fig. 6B). Ligand-binding affinities were slightly reduced, a finding consistent with the reduced affinity of other dimerization-defective sEGFR mutants. However, none of the mutations reduced EGF or TGF-α binding affinity by more than 4.2-fold (see legend to Fig. 6B). Thus, the lack of dimerization of these mutants does not reflect a loss of ligand binding but rather argues that the domain II/III buttressing interactions play an important role in ligand-induced receptor dimerization.

Conclusions. By analyzing sEGFR mutants we found that domain IV interactions contribute very little (<9%) to dimerization, and that over 75% of the sEGFR dimerization energy is contributed by the domain II dimerization arm plus a single adjacent loop (in disulfide-bonded module 6) that contains D279 and H280 (Fig. 5A). Each of these contact points is fully occluded by the intramolecular domain II/IV tether in monomeric sEGFR (12), as depicted in the diagram presented in Fig. 5B. Ligand binding to the receptor does more than simply expose this region, actually altering the conformation of domain II to maximize cooperation between dimer contact sites in the fifth and sixth disulfide-bonded modules (Fig. 1C and 5A). Our results suggest that three key residues in domains II and III (N274, E293, and R405) allow domain III in the ligand-occupied receptor to act as a buttress that projects module 6 of domain II (including D279/H280) further into the dimerization interface, thus maximizing intermolecular contacts and promoting dimerization. This buttressing of the C-terminal region of domain II by domain III is seen in both the dimeric sEGFR structures (17, 24) and sErbB2 structures (9, 14, 16), and we suggest that it is responsible for the transition from the inactive (red/magenta) to active (blue/cyan) domain II configurations shown in Fig. 1C. In the model presented in Fig. 5B, this effect is exaggerated to suggest that the domain III buttress effectively creates an additional dimerization site in the C-terminal part of domain II.

This model may help to explain several unanswered questions regarding ErbB receptor homo- and heterodimerization. First, it explains why exposure of the dimerization arm is not sufficient for EGFR dimerization. An additional conformational rearrangement in the C-terminal part of domain II must also be induced in order to promote receptor dimerization (Fig. 5B). Second, our findings may help to explain why ErbB3 and ErbB2 fail to homodimerize (4, 6, 13), despite sharing the majority of the key dimerization arm residues with EGFR, but instead form heterodimers. Regions outside the dimerization arm must play a key role in determining homo- versus heterodimerization specificity. In the case of EGFR, module 6 (buttressed by domain III) appears to provide the additional (self-complementary) interactions (including D279 and H280) that allow efficient homodimerization. For ErbB2/ErbB3 heterodimer formation, mutational studies by Franklin et al. (14) showed that disulfide-bonded module 7 plays a key role, and this region may provide the additional (mutually complementary) interactions required for these two receptors to associate in heteromer. Interestingly, the key residues involved in the domain III/II contacts that buttress disulfide-bonded modules 6 and 7 (i.e., N274, E293, and R405 in EGFR) are conserved

in all four human ErbB receptors. Moreover, all of the domain III/II interactions shown in Fig. 5A for sEGFR are conserved in the available structures of the constitutively extended ErbB2 extracellular region (9, 14, 16).

Finally, one intriguing possibility raised by these suggestions is that different ErbB ligands could induce distinct (but similar) domain III positions, leading to subtly different configurations of the domain II C terminus in a particular receptor. If this is true, different ErbB ligands could potentially stabilize extended forms of their receptors with slightly altered homo- and heterodimerization specificities, and this could contribute to their distinct signaling specificities (2).

ACKNOWLEDGMENTS

We thank members of the Lemmon, Ferguson, and Schlessinger laboratories for valuable discussions and critical comments on the manuscript and Shigeyuki Yokoyama for communicating results prior to publication.

This study was supported in part by NIH grants R01-CA079992 (to M.A.L.), R01-AR051448 (to J.S.), and K01-CA092246 (to K.M.F.); a predoctoral fellowship DAMD17-98-1-8232 from the U.S. Army Breast Cancer Research Program (to M.B.B.); a postdoctoral fellowship (PF-04-123-01-GMC) from the American Cancer Society (to J.P.D.); and a Career Award in the Biomedical Sciences from the Burroughs Wellcome Fund (to K.M.F.).

REFERENCES

1. **Arteaga, C. L.** 2003. ErbB-targeted therapeutic approaches in human cancer. Exp. Cell Res. **284:**122–130.
2. **Beerli, R. R., and N. E. Hynes.** 1996. Epidermal growth factor-related peptides activate distinct subsets of ErbB receptors and differ in their biological activities. J. Biol. Chem. **271:**6071–6076.
3. **Berezov, A., J. Chen, Q. Liu, H. T. Zhang, M. I. Greene, and R. Murali.** 2002. Disabling receptor ensembles with rationally designed interface peptidomimetics. J. Biol. Chem. **277:**28330–28339.
4. **Berger, M. B., J. M. Mendrola, and M. A. Lemmon.** 2004. ErbB3/HER3 does not homodimerize upon neuregulin binding at the cell surface. FEBS Lett. **569:**332–336.
5. **Blume-Jensen, P., and T. Hunter.** 2001. Oncogenic kinase signaling. Nature **411:**355–365.
6. **Burgess, A. W., H.-S. Cho, C. Eigenbrot, K. M. Ferguson, T. P. J. Garrett, D. J. Leahy, M. A. Lemmon, M. X. Sliwkowski, C. W. Ward, and S. Yokoyama.** 2003. An open-and-shut case? Recent insights into the activation of EGF/ErbB receptors. Mol. Cell **12:**541–552.
7. **Cantor, C. R., and P. R. Schimmel.** 1980. Biophysical chemistry: techniques for the study of biological structure and function. W. H. Freeman, New York, N.Y.
8. **Cho, H. S., and D. J. Leahy.** 2002. Structure of the extracellular region of HER3 reveals an interdomain tether. Science **297:**1330–1333.
9. **Cho, H. S., K. Mason, K. X. Ramyar, A. M. Stanley, S. B. Gabelli, D. W. Denney, Jr., and D. J. Leahy.** 2003. Structure of the extracellular region of HER2 alone and in complex with the Herceptin Fab. Nature **421:**756–760.
10. **Dancey, J. E.** 2004. Predictive factors for epidermal growth factor receptor inhibitors: the bull's-eye hits the arrow. Cancer Cell **5:**411–415.
11. **Elleman, T. C., T. Domagala, N. M. McKern, M. Nerrie, B. Lonnqvist, T. E. Adams, J. Lewis, G. O. Lovrecz, P. A. Hoyne, K. M. Richards, G. J. Howlett, J. Rothacker, R. N. Jorissen, M. Lou, T. P. Garrett, A. W. Burgess, E. C. Nice, and C. W. Ward.** 2001. Identification of a determinant of epidermal growth factor receptor ligand-binding specificity using a truncated, high-affinity form of the ectodomain. Biochemistry **40:**8930–8939.
12. **Ferguson, K. M., M. B. Berger, J. M. Mendrola, H. S. Cho, D. J. Leahy, and M. A. Lemmon.** 2003. EGF activates its receptor by removing interactions that autoinhibit ectodomain dimerization. Mol. Cell **11:**507–517.
13. **Ferguson, K. M., P. J. Darling, M. J. Mohan, T. L. Macatee, and M. A. Lemmon.** 2000. Extracellular domains drive homo- but not heterodimerization of erbB receptors. EMBO J. **19:**4632–4643.
14. **Franklin, M. C., K. D. Carey, F. F. Vajdos, D. J. Leahy, A. M. de Vos, and M. X. Sliwkowski.** 2004. Insights into ErbB signaling from the structure of the ErbB2-pertuzumab complex. Cancer Cell **5:**317–328.
15. **Fry, D. W.** 2003. Mechanism of action of erbB tyrosine kinase inhibitors. Exp. Cell Res. **284:**131–139.
16. **Garrett, T. P. J., N. M. McKern, M. Lou, T. C. Elleman, T. E. Adams, G. O. Lovrecz, M. Kofler, R. N. Jorissen, E. C. Nice, A. W. Burgess, and C. W. Ward.** 2003. The crystal structure of a truncated ErbB2 ectodomain reveals an active conformation, poised to interact with other ErbB receptors. Mol. Cell **11:**495–505.
17. **Garrett, T. P. J., N. M. McKern, M. Lou, T. C. Elleman, T. E. Adams, G. O. Lovrecz, H. J. Zhu, F. Walker, M. J. Frenkel, P. A. Hoyne, R. N. Jorissen, E. C. Nice, A. W. Burgess, and C. W. Ward.** 2002. Crystal structure of a truncated epidermal growth factor receptor extracellular domain bound to transforming growth factor alpha. Cell **110:**763–773.
18. **Gorgoulis, V., D. Aninos, P. Mikou, P. Kanavaros, A. Karameris, J. Joardanoglou, A. Rasidakis, M. Veslemes, B. Ozanne, and D. A. Spandidos.** 1992. Expression of EGF, TGF–alpha and EGFR in squamous cell lung carcinomas. Anticancer Res. **12:**1183–1187.
19. **Lemmon, M. A., Z. Bu, J. E. Ladbury, M. Zhou, D. Pinchasi, I. Lax, D. M. Engelman, and J. Schlessinger.** 1997. Two EGF molecules contribute additively to stabilization of the EGFR dimer. EMBO J. **16:**281–294.
20. **Libermann, T. A., H. R. Nusbaum, N. Razon, R. Kris, I. Lax, H. Soreq, N. Whittle, M. D. Waterfield, A. Ullrich, and J. Schlessinger.** 1985. Amplification, enhanced expression and possible rearrangement of EGF receptor gene in primary human brain tumours of glial origin. Nature **313:**144–147.
21. **Libermann, T. A., N. Razon, A. D. Bartal, Y. Yarden, J. Schlessinger, and H. Soreq.** 1984. Expression of epidermal growth factor receptors in human brain tumors. Cancer Res. **44:**753–760.
22. **Mattoon, D., P. Klein, M. A. Lemmon, I. Lax, and J. Schlessinger.** 2004. The tethered configuration of the EGF receptor extracellular domain exerts only a limited control of receptor function. Proc. Natl. Acad. Sci. USA **101:**923–928.
23. **Odaka, M., D. Kohda, I. Lax, and J. Schlessinger.** 1997. Ligand-binding enhances the affinity of dimerization of the extracellular domain of the epidermal growth factor receptor. J. Biochem. **122:**116–121.
24. **Ogiso, H., R. Ishitani, O. Nureki, S. Fukai, M. Yamanaka, J. H. Kim, K. Saito, A. Sakamoto, M. Inoue, M. Shirouzu, and S. Yokoyama.** 2002. Crystal structure of the complex of human epidermal growth factor and receptor extracellular domains. Cell **110:**775–787.
25. **Ranson, M., and M. X. Sliwkowski.** 2002. Perspectives on anti-HER monoclonal antibodies. Oncology **63**(Suppl. 1)**:**17–24.
26. **Salomon, D. S., R. Brandt, F. Ciardiello, and N. Normanno.** 1995. Epidermal growth factor-related peptides and their receptors in human malignancies. Crit. Rev. Oncol. Hematol. **19:**183–232.
27. **Schlessinger, J.** 2000. Cell signaling by receptor tyrosine kinases. Cell **103:** 211–225.
28. **Schlessinger, J.** 2003. Signal transduction. Autoinhibition control. Science **300:**750–752.
29. **Slamon, D. J., G. M. Clark, S. G. Wong, W. J. Levin, A. Ullrich, and W. L. McGuire.** 1987. Human breast cancer: correlation of relapse and survival with amplification of the HER-2/neu oncogene. Science **235:**177–182.
30. **Ullrich, A., and J. Schlessinger.** 1990. Signal transduction by receptors with tyrosine kinase activity. Cell **61:**203–212.
31. **Walker, F., S. G. Orchard, R. N. Jorissen, N. E. Hall, H. H. Zhang, P. A. Hoyne, T. E. Adams, T. G. Johns, C. Ward, T. P. Garrett, H. J. Zhu, M. Nerrie, A. M. Scott, E. C. Nice, and A. W. Burgess.** 2004. CR1/CR2 interactions modulate the functions of the cell surface epidermal growth factor receptor. J. Biol. Chem. **279:**22387–22398.
32. **Yarden, Y., and M. X. Sliwkowski.** 2001. Untangling the ErbB signalling network. Nat. Rev. Mol. Cell. Biol. **2:**127–137.